

# Optimal design of multilayered polysilicon films for prescribed curvature

A. NI, D. SHERMAN, R. BALLARINI, H. KAHN, B. MI, S. M. PHILLIPS,  
A. H. HEUER

Case Western Reserve University, Cleveland, Ohio 44106, USA

LPCVD polysilicon films exhibit tensile or compressive residual stresses and stress gradients, depending on deposition temperature. The stresses, which are a result of an “intrinsic” growth eigenstrain,  $\varepsilon^g$ , produce undesired curvatures in released structures. A combined experimental/computational design procedure is presented for controlling the curvature of thin films comprised of tensile layers, deposited at 570°C, alternated with compressive layers deposited at 615°C. Experimental measurements are first used to calculate the through-the-thickness variation of  $\varepsilon^g$  for both temperatures. This information is in turn incorporated into a mechanical model that predicts, for prescribed parameters that define the geometry, elastic moduli, and eigenstrain distribution, the stress distribution before release, and the curvature upon release, of multilayered films. Comparisons of predicted and measured average stress before release of a number of films, and of the curvature upon release of a circular micromirror device, provide a preliminary assessment of the semi-empirical model, which when combined with optimization algorithms can be used to develop recipes (thicknesses of the individual layers of a multiplayer device) that will achieve prescribed curvature according to given constraints.

© 2003 Kluwer Academic Publishers

## 1. Introduction

As the most widely used structural material for surface-micromachined MEMS (microelectromechanical systems) devices, polysilicon is typically deposited by LPCVD using silane ( $\text{SiH}_4$ ). Deposition conditions, especially the deposition temperature, significantly affect the microstructure of LPCVD polysilicon films. Amorphous films with smooth surfaces are formed when the growth temperature is lower than  $\sim 560^\circ\text{C}$ . Crystalline films (formed by crystallization (“devitrification”) of an initially amorphous deposit) with fine ellipsoidal grains and smooth surfaces, are formed with growth temperature in the range from  $\sim 560^\circ\text{C}$  to  $\sim 600^\circ\text{C}$ . Films with columnar (110)-textured grains with rougher surfaces are obtained for temperatures ranging from  $\sim 610^\circ\text{C}$  to  $\sim 700^\circ\text{C}$  [1].

Depending on these deposition temperatures, LPCVD polysilicon films exhibit tensile or compressive residual stresses and stress gradients; compressive stress is present in the amorphous and the columnar films, while tensile stress is present in the devitrified fine-grained films [1–3]. Upon release, a film that is not annealed suffers from undesired out-of-plane displacements and an associated curvature. Fig. 1 is a micrograph of the individual combs of a comb-drive actuator of a MEMS device, whose performance is severely compromised by such an out of plane deformation.

Such undesired curvatures upon release can be prevented without annealing through the *MultiPoly*

fabrication process [1]; this is achieved by alternating layers deposited at  $570^\circ$  and  $615^\circ$  (Fig. 2). The result is a multilayer film that can be engineered to have zero average stress and an overall zero stress gradient. Fig. 3a shows a series of long and relatively flat cantilevers fabricated using this process. It is observed that this empirically developed recipe (9 layers with thickness values, in  $\mu\text{m}$ , starting with the first  $570^\circ\text{C}$  layer, 0.49, 0.66, 0.56, 0.34, 0.72, 0.50, 0.41, 0.46, 0.46) involves a curvature, as evidenced by the downward deflection of the free (left) ends of the beams. Using the empirical approach, this relatively small curvature is eliminated, as shown in Fig. 3b, by adding additional compensating stresses through a (thin)  $0.1 \mu\text{m}$ ,  $570^\circ\text{C}$  correction layer.

Obviously the empirical approach is not practical for developing the recipes required to achieve desired curvatures of films of prescribed total thickness and number of layers. This paper presents the preliminary results obtained using a semi-empirical design procedure for developing such recipes through the combination of laminate theory, experimental measurements of growth eigenstrains in films formed at  $570^\circ$  and  $615^\circ$ , and a direct search optimization algorithm. The paper presents, in the following order, the laminate theory, experimental determination of the growth eigenstrains, a comparison of the model’s predictions with those of several MEMS devices, and suggestions for improving the robustness of the design procedure.

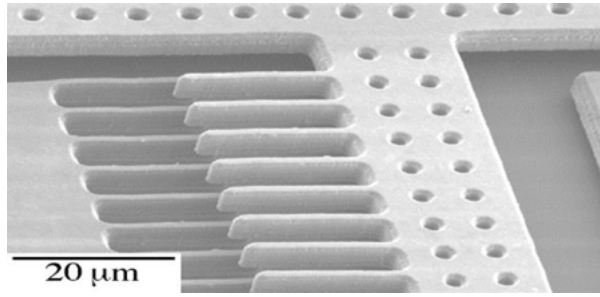


Figure 1 Micrograph of portion of the comb drive actuator of a MEMS device, showing undesired out of plane deformation.

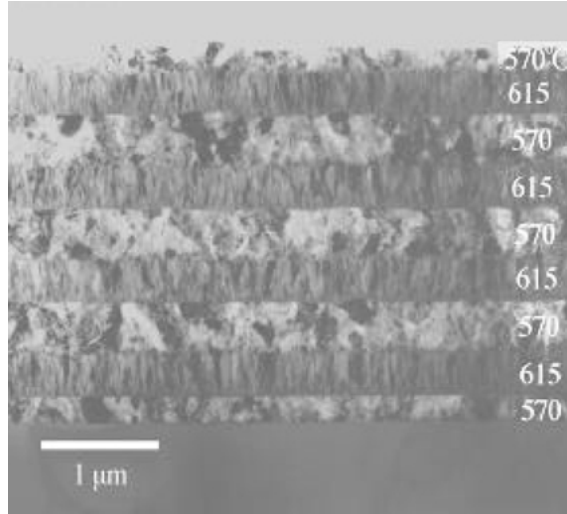


Figure 2 Cross-section of nine layer MultiPoly film.

**2. Structural mechanics of multilayer films**

Consider a linear elastic laminated plate comprised of  $n$  layers, each denoted by subscript  $i$ , of thickness  $h_i$ , Young’s modulus  $E_i$ , Poisson’s ratio  $\nu_i$ , and coefficient of thermal expansion  $\alpha_i$ . The internal stresses in the  $i$ th layer result from the difference in thermal eigenstrains,  $\epsilon_i^t = \alpha_i \Delta T_i$ , between the layers, and the eigenstrain due

to growth within the layers,  $\epsilon_i^g$ . It is important to note that  $\epsilon_i^g$ , which varies across the thickness of individual films, is to be determined experimentally. Thus the total eigenstrain is written

$$\epsilon_i^m = \epsilon_i^t + \epsilon_i^g \tag{1}$$

As shown in Fig. 4, the per unit thickness force and moment resultants in the  $i$ th layer are defined as  $P_i$  and  $M_i$ , respectively. Edge effects are neglected, and the assumption of an equal biaxial stress state is assumed. Force and moment equilibria of the laminate provide

$$\sum_{i=1}^n P_i = 0 \tag{2}$$

and

$$\sum_{i=1}^n M_i - \sum_{i=1}^{n-1} P_i \left[ \frac{h_i + h_n}{2} + \sum_{k=i+1}^{n-1} h_k \right] = 0 \tag{3}$$

The moments are related to the curvatures,  $\kappa_i$ , through the relation

$$M_i = \kappa_i D_i (1 + \nu_i) \tag{4}$$

where  $D_i = E_i h_i^3 / 12(1 - \nu_i^2)$  is the bending rigidity. Compatibility demands a uniform curvature  $\kappa$ , and continuous axial strain along the  $n - 1$  interfaces

$$\epsilon_{i-1}^m + \frac{P_{i-1}}{E'_{i-1} h_{i-1}} + \frac{h_{i-1} \kappa}{2} = \epsilon_i^m + \frac{P_i}{E'_i h_i} - \frac{h_i \kappa}{2} \tag{5}$$

Equations 2–5 represent  $2n + 1$  equations that relate the  $n$  forces,  $n$  moments, and the curvature to the through-the-thickness variation of eigenstrain. Once these are solved, the residual stress distribution before release can be recovered as

$$\sigma_i = \frac{P_i}{h_i} + \frac{h_i E'_i}{2} \kappa \tag{6}$$

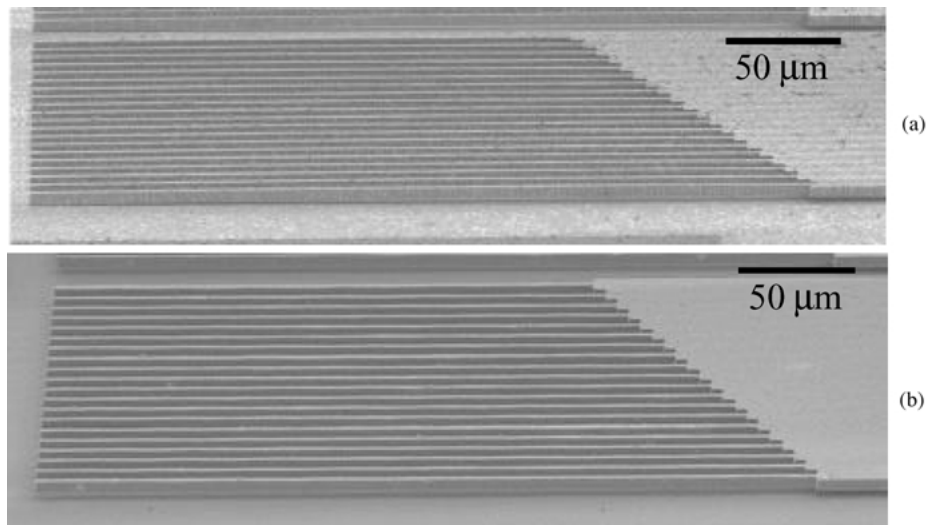


Figure 3 Cantilever beams fabricated using MultiPoly process.

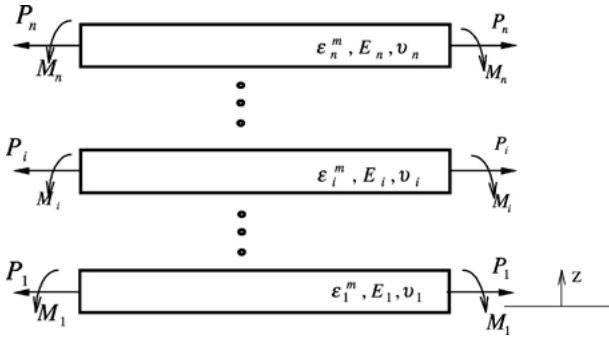


Figure 4 Free body diagrams of individual layers of laminated films.

### 3. Experimental/theoretical measurement of growth eigenstrain functions

The ideal method for deriving the through thickness distribution of growth eigenstrain involves measuring, on a large number of different thickness films, the curvature of the film/substrate composite. Each measurement would provide, through the application of the laminate theory described above, one point on the eigenstrain-thickness function. Also, structures can be made from the films that are released from the substrates. The curvatures of these structures will give the overall stress gradient of the film. Instead of this time-consuming procedure, the following short-cut is investigated. One single film is fabricated, and the curvature of the film-substrate is measured as its thickness is etched away in small increments. Laminate theory is in turn used to determine the eigenstrain-thickness function.

The details are as follows. 500  $\mu\text{m}$  thick (100) silicon substrates were oxidized at 1075°C to grow 100 nm thick films of  $\text{SiO}_2$ . Thereafter, 2  $\mu\text{m}$  thick LPCVD polysilicon films were deposited on both sides, and the polysilicon layer was stripped off one side using a chlorine plasma. A schematic drawing of the resulting structure is shown as Fig. 5. The two polysilicon deposition temperatures were 615°C and 570°C. The 570°C films were annealed directly after deposition for two hours at 615°C to ensure complete crystallization of the initially amorphous deposit. All curvature measurements were taken at room temperature.

Determination of the eigenstrains,  $\epsilon_i^m$ , for the polysilicon films relies on the measured curvature history of this  $\text{SiO}_2/\text{Si}/\text{SiO}_2/\text{poly-Si}$  structure, as the polysilicon layer is etched in roughly 100 nm increments. The radius of curvature as a function of the polysilicon film thickness is shown in Fig. 6 for both deposition temperatures.

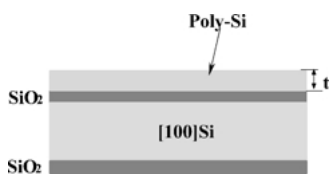


Figure 5 Schematic drawing of experimental configuration used to determine the distribution of growth eigenstrain. The thickness of the single crystal substrate is 500  $\mu\text{m}$ , that of both oxide layers is 0.1  $\mu\text{m}$ . The as-processed thickness of the polysilicon is 2.0  $\mu\text{m}$ .

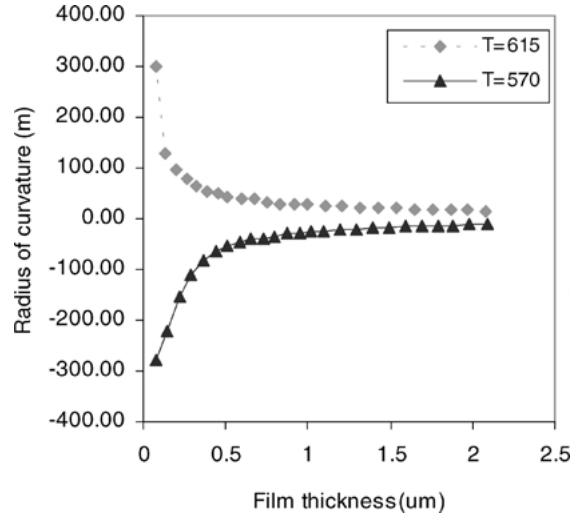


Figure 6 Radius of curvature as a function of film thickness.

The material properties of silicon,  $\text{SiO}_2$ , and polysilicon used for the analysis are shown in Table I, together with the change in temperature and thermal mismatch strain of each layer during fabrication. The  $\text{SiO}_2$  layers are assumed to contain no growth strains at the deposition temperature; the coefficient of thermal expansion for Si and  $\text{SiO}_2$  are assumed to be independent of temperature, and the curvature of the  $\text{SiO}_2/\text{Si}/\text{SiO}_2$  composite before polysilicon deposition is assumed to be zero. Even if these assumptions are incorrect, they have little effect on subsequent calculations.

For computational convenience,  $\epsilon_i^m(z)$  was calculated by adding, rather than removing, the polysilicon layer. In other words, the configuration corresponding to the last etching step was treated as the initial configuration. This configuration consists of four layers ( $n = 4$ ), the two  $\text{SiO}_2$  layers, the single crystal silicon layer, and the final polysilicon layer. The magnitude of the eigenstrain within this thin layer is assumed uniform across the thickness, and is calculated, using Equations 2–5, to be consistent with the measured curvature. This procedure is repeated as the layers are added back, so that in the next step, the added layer becomes the fifth layer ( $n = 5$ ) of the laminate, and the corresponding curvature is used to calculate the magnitude of the eigenstrain through its thickness. The results of this repeated process are shown in Fig. 7, which clearly shows that the growth stresses are not uniform through the thickness.

The stress distribution in the film before etching is shown in Fig. 8. As expected, when polysilicon is deposited at 570°C, it is under tension, while when it is deposited at 615°C, it is under compression.

TABLE I Relevant data for Si,  $\text{SiO}_2$  and polysilicon used in the analysis

	$E$ (GPa)	$\nu$	$\alpha$ ( $10^{-6}/^\circ\text{C}$ )	$\Delta T$ ( $^\circ\text{C}$ )	$\epsilon^m(z)$
Si	144	0.22	2.5	-1050	$-2.63 \times 10^{-3}$
$\text{SiO}_2$	70	0.25	0.5	-1050	$-5.25 \times 10^{-3}$
Poly-Si	160	0.22	2.5	-590 -545	Calculated for each temperature

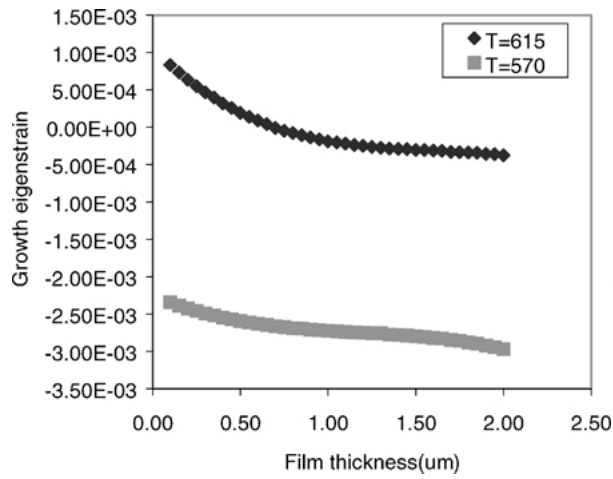


Figure 7 Through-the-thickness variation in growth eigenstrain in the polysilicon film.

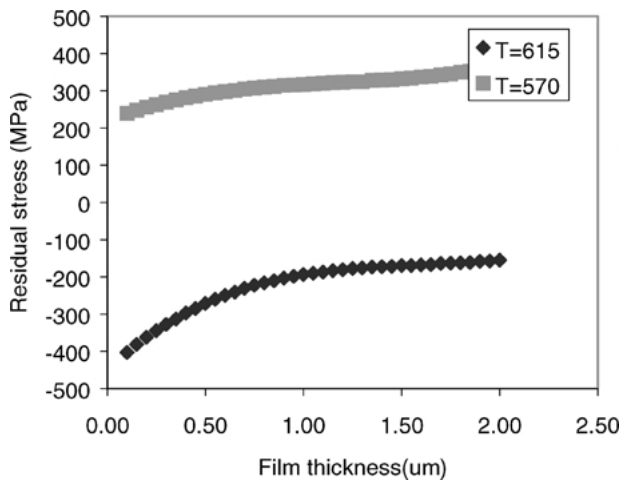


Figure 8 Residual stresses in (unreleased) film.

**4. Assessment of the derived eigenstrain functions**

In this section we present the results obtained when the experimentally measured eigenstrain functions are used to predict the curvature and stress distribution in multilayer films. At this point in time we can conduct only a preliminary assessment of the procedure because

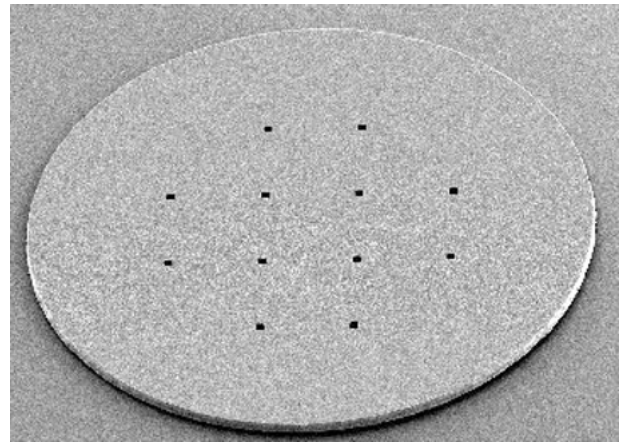


Figure 9 SEM micrograph of 300 μm diameter micromirror device.

insufficient data is available for the curvature upon release and the residual stress before release of multilayer films.

What is available to us includes the curvature of a 300 μm diameter micromirror (Fig. 9). The 5 μm thick film is comprised of 8 layers, with individual layer thicknesses (starting with 615°C) of 0.5, 1.0, 0.3, 1.0, 0.35, 0.75, 0.5, and 0.6 μm. The radius of curvature measured using optical interferometry was 8.57 mm, and the predicted radius of 8.3 mm is encouraging.

Table II lists 8 different recipes for which the average residual stress before release was measured using pointer beams described by Kahn *et al.* [3]. The predicted average stresses are compared with the experimental measurements in Fig. 10. It appears that except for the very good agreement of the first two films, the design procedure overestimates the residual stress. This is not surprising; the curvature and residual stress in a multilayer film is sensitive to the eigenstrain functions. The short-cut experimental procedure presented in this paper obviously does not lead to an accurate enough representation of these functions. The largest source of error is likely the assumption that the incremental removal of each polysilicon layer was uniform across the film. The removal rate probably varied by ~5% between the center and the edges of the film. The

TABLE II Recipes of 8 multilayer films. S indicates top surface, and I indicates interface

		Samples							
Total film thickness (μm)		4.05	3	1.96	4.59	4.69	4.21	3.72	3.12
No. of layers	Deposition temperature (°C)	8	5	5	9	10	9	9	8
	S					0.10			
	570				0.46	0.46	0.53	0.48	0.48
	615	0.45			0.46	0.46	0.41	0.21	0.31
	570	0.70			0.41	0.41	0.36	0.43	0.52
	615	0.20			0.50	0.50	0.44	0.24	0.22
	570	0.70	0.71	0.28	0.71	0.71	0.64	0.79	0.52
	615	0.65	0.66	0.59	0.34	0.34	0.30	0.16	0.24
	570	0.25	0.59	0.24	0.56	0.56	0.50	0.58	0.52
	615	0.65	0.70	0.50	0.66	0.66	0.59	0.32	0.31
	I	0.45	0.34	0.35	0.49	0.49	0.44	0.51	

TABLE III Optimal recipe for 5  $\mu\text{m}$  thick 9 layer flat and curved films. The odd layers are deposited at 570°C, the even at 615°C.

Layer no.	Layer thickness ( $\mu\text{m}$ )									Total thick ( $\mu\text{m}$ )
	1	2	3	4	5	6	7	8	9	
Curved	0.88	0.23	0.89	0.48	0.46	0.77	0.18	0.93	0.18	5.0
Flat	0.55	0.55	0.57	0.56	0.54	0.57	0.57	0.57	0.53	5.0

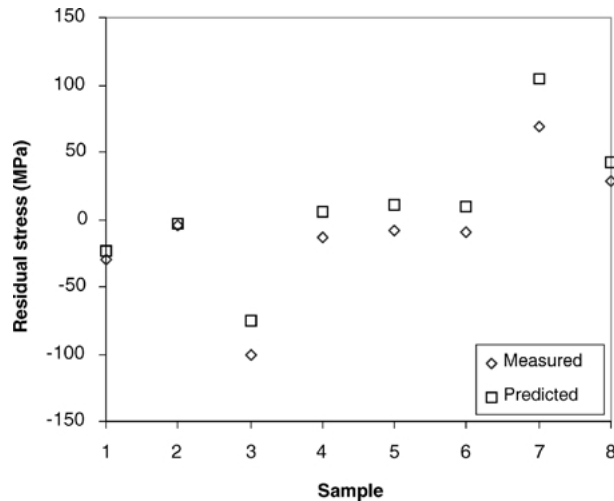


Figure 10 Comparison of measured and predicted average residual stress in 8 different multilayer films.

procedure could be made more robust by perturbing the derived eigenstrain functions so that the discrepancies shown in Fig. 10 are reduced to acceptable levels. Furthermore, a series of the previously discussed time-consuming one specimen procedure for determining the eigenstrain functions should be performed. These additional experiments will clearly demonstrate whether the short-cut procedure is adequate.

If the semi-empirical model is made robust, it could be used as the backbone of an optimization algorithm that calculates recipes for prescribed curvatures in minimum amount of fabrication time. Table III shows, for illustrative purposes, two solutions obtained using the derived eigenstrain functions and a direct search method for 9 layer 5  $\mu\text{m}$  films with prescribed curva-

ture and minimum time in the fabrication laboratory (the deposition rates are not presented here).

## 5. Summary and conclusion

A semi-empirical procedure for designing the curvature of multilayered thin film devices was introduced. This tool relies on an experimental procedure to determine the eigenstrains associated with the growth of polysilicon films deposited at 570°C and 615°C, a mechanical laminate analysis, and an optimization procedure. A preliminary assessment of the model was made by comparing the predicted and experimentally measured curvatures and average residual stresses of several MEMS devices, and yielded fair agreement. Additional experimental and theoretical work is required to determine whether the growth eigenstrain functions are universal, and how sensitive the predictions are to the relevant input parameters.

Recent data obtained using the one specimen procedure discussed above indicate that the short-cut experimental procedure produces results that are equivalent within the experimental measurement error; for both techniques, care must be taken to ensure proper evaluation at the smallest film thicknesses.

## Acknowledgement

This work was partially supported by DARPA, under contract N00014-00-1-0881 and the Glennan Microsystems Initiative.

## References

1. J. YANG, H. KAHN, A. HE, S. M. PHILLIPS and A. H. HEUER, *IEEE Journal of Microelectromech. Syste.* **9**(4) (2000) 485.
2. P. TEMPLE-BOYER, E. IMBERNON, B. ROUSSET and E. SCHEID, *Mater. Res. Soc. Symp. Proc.* **518** (1998) 209.
3. H. KAHN, S. STEMMER, K. NANDAKUMAR, A. H. HEUER, R. L. MULLEN, R. BALLARINI and M. A. HUFF, "Mechanical Properties of Relatively Thick, Surface Micro-machined Polysilicon Films," in Proceedings, IEEE The Ninth Annual International Workshop on Micro Electro Mechanical Systems, San Diego, California, Feb. 11–15, 1996, p. 343.